Mater. Res. Soc. Symp. Proc. Vol. 1770 © 2015 Materials Research Society
DOI: 10.1557/opl.2015.727

Observation of Superheating of Si at the Si/SiO_2 Interface in Pulsed-laser irradiated Si Thin Films

J.J. Wang, A.B. Limanov, Ying Wang, and James S. Im

Materials Science and Engineering, Department of Applied Physics and Applied Mathematics, Columbia University, New York, NY, USA

ABSTRACT

Substantial superheating of single-crystal Si films at and near the bottom Si/SiO_2 interface was observed. This was accomplished via back-side irradiation of a (100) single-crystal Si film on a quartz substrate using an excimer-laser pulse. The spatiotemporal details of the melting transition were tracked *in situ* using surface-side and substrate-side transient reflectance measurements, and the one-dimensional thermal profile evolution within the solid film during the heating period was numerically computed using the experimentally extracted temporal profile of the incident beam and temperature-dependent optical and thermal parameters of the materials. A simple lower-bound estimation identifies that superheating in excess of 100 K was attained within Si along the bottom (100)-Si/SiO_2 interface even at moderate beam energy densities.

INTRODUCTION

The extent to which melting proceeds in laser irradiated Si films has long been recognized as the singularly critical factor that determines the ensuing solidification scenario in laser-induced melt-mediated crystallization of the films [1]. For partial-melting-based laser-crystallization approaches [1-5], it is becoming even more evident that the specific details associated with the initial formation and subsequent growth of the liquid phase in the polycrystalline Si films essentially dictate the ensuing microstructural changes that take place in the films; this is the case for excimer laser annealing (ELA) employed in the manufacture of advanced LCDs and OLED displays, as well as for the mixed-phase-solidification (MPS) method [4], which can create large-grained, (100)-surface-textured Si on SiO_2 for photovoltaic and microelectronic applications [6]. In other words, we suggest that for these multiple-exposure-based techniques, the melting period corresponds to the all-significant processing phase in that it (1) determines the incremental increase in the average grain size [3] and (2) affects the gradual development of the surface orientation texture [4,7], provided, of course, that nucleation is avoided [1,8]. The established principles of discontinuous phase transitions point to various extrinsic excess free energy sites in polycrystalline Si films (e.g., surfaces, grain boundaries, dislocations, and Si/SiO_2 interfaces), along with the Gibbs-Thomson effect [9,10], as the key elements and factors that will dictate spatially and temporally heterogeneous initiation and propagation of the melt in the films [11]. Understanding such details may, therefore, lead to further optimization of, and advances in, these and other partial-melting-based laser crystallization techniques.

In this paper, we present preliminary results obtained from experiments on excimer-laser-induced melting of Si films on SiO_2. By utilizing an unconventional combination of sample configuration and experimental capabilities, we have succeeded in inducing and detecting superheating of Si films at and near the Si/SiO_2 interface. While the present work is driven primarily by the motivation to understand and improve the aforementioned laser crystallization

methods, we also recognize that there exists an opportunity to contribute scientifically in providing much desired experimental results in the long-investigated topic of melting [11,12]; here, due to the pervasive and prompt participation of surface melting at or near the equilibrium point as the samples are typically externally heated, experimental investigations of melting transpiring in superheated solids, especially involving simple materials (e.g., single-component system, single-crystal microstructure, planar surfaces and interfaces, etc.), have been rather lacking [12].

EXPERIMENTAL

In this work, we leverage the following sample configurations and experimental capabilities for the purpose of inducing and detecting superheating in excimer-laser-irradiated Si films: (1) (100)-oriented single-crystal Si on quartz, (2) back-side irradiation of the sample through the transparent substrate, and (3) *in situ* surface-side and substrate-side transient reflectance (TR) [13]. The single-crystal material with (100) surface orientation was chosen for investigation as the material is, first and foremost, free of grain boundaries (thereby enabling us to focus on simpler and uniform excess free energy sites of the top surface and the bottom Si/SiO_2 interface); and, additionally, the (100) Si/SiO_2 interface corresponds presumably to the most energetically stable configuration [14] (thereby making this interface commensurately more melt-resistant than those of other orientations). The transparent nature of quartz is a particularly and doubly enabling element in the present experiment as it permitted us to (1) back-side irradiate the sample and induce internal heating of the film via subsurface energy deposition of the incident beam mostly near the bottom interface, and (2) obtain more spatially comprehensive *in situ* information about how melting proceeds in the film by examining the substrate-side TR signals (in addition to the usual surface-side TR signals).

The samples utilized in the present investigation consisted of 200-nm (100)-oriented undoped Si on thermal SiO_2 on quartz (manufactured via a wafer-bonding-based Si-on-insulator (SOI) fabrication technique). Initially, the samples were coated with a thin capping oxide layer deposited using low-pressure chemical vapor deposition (LPCVD); BHF-etchant was utilized to completely remove the oxide layer just moments prior to being irradiated. The samples were single-shot back-side irradiated (i.e., the substrate-side through the transparent quartz substrate) at various energy densities (up to ~2.5 CMT (complete melting threshold) or 1.6 J/cm^2) at normal incidence using a 308-nm XeCl excimer laser pulse (see Figure 1(b) for the experimentally extracted temporal profile of the beam). The beam was spatially homogenized, shaped, de-magnified, and imaged onto a 1 x 1 mm^2 area on the sample. The laser pulse energy was monitored using a calibrated energy meter, which received a fraction of the excimer laser light from a beam splitter. All of the laser irradiation experiments in this study were performed under ambient conditions. *In situ* surface-side and substrate-side transient reflectance (TR) were measured using two 670-nm diode lasers at incident angles of 50° (with respect to the surface normal) and detected using Si diodes with less than 1 ns rise times. The probe laser beams were focused down to a diameter of about 0.2 mm on the film.

RESULTS

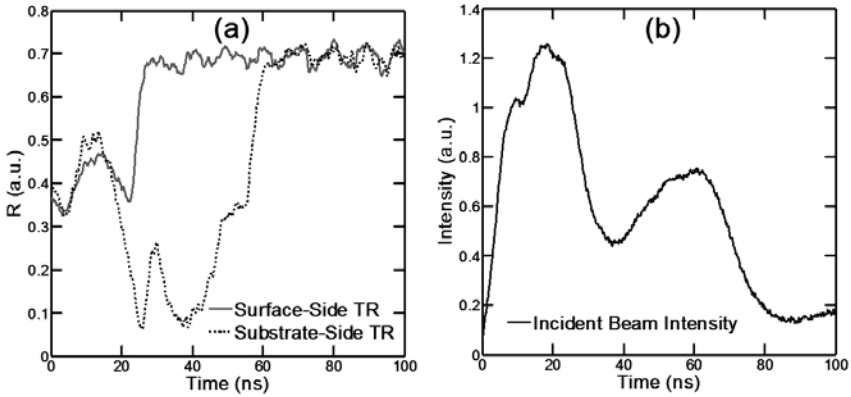

Figure 1: (a) *In situ* surface-side and substrate-side transient reflectance (TR) measured at 670 nm at incident angles of 50° during back-side excimer-laser irradiation of the Si film at 800 mJ/cm^2 or 1.2 CMT. The initial peak in both TR signals is caused by simple solid phase heating of the film. (b) Experimentally extracted time-dependent intensity profile of the incident excimer laser beam.

Figure 1(a) shows a representative set of surface-side and substrate-side TR signals when the BHF-etched Si film was back-side irradiated with a laser pulse at an energy density that is well within the complete-melting regime. When interpreting TR signals, one must at least consider the effects that arise from (1) the higher reflectivity of metallic liquid Si than that of semiconducting solid Si [13], and (2) the thin-film interference [15] resulting from the creation and movement of the solid/liquid interface [16]. More specifically, we note that, for the wavelength and incident angle of the probe laser beams in this experiment, the reflectance signals obtained from the side from which melting initiates and propagates must saturate when the thickness of the liquid Si layer exceeds ~20 nm. Based upon these established considerations, it is possible to deduce from the TR signals shown in Figure 1(a) that melting initiated and propagated from the top surface. Figure 1(b) shows the measured time-dependent intensity profile of the incident excimer laser pulse.

ANALYSIS AND DISCUSSION

We suggest that the observation of the occurrence of surface melting in the irradiated films (as depicted in Figure 1(a)) corresponds to the most notable outcome of the present work; it indicates immediately that superheating must have transpired within the Si film. Specifically, a consideration of the energy deposition profile and subsequent heat flow encountered during the back-side-irradiation-induced heating of the film leads one to conclude that the surface temperature, at least whilst it rises, must be the lowest within the film (i.e., during the heating phase while the intense beam is still incident on the sample). Thus, when one additionally considers the fact that the free surface of solid Si is expected to essentially melt at (or at least quite near) the equilibrium transition temperature, one can deduce from the observation that

definite superheating of the film must have taken place particularly significantly at and near the bottom interface (starting at some point before surface melting was initiated and lasting up until the region is converted into liquid via the advancing melting interface originating heterogeneously from the surface).

In fact, by taking advantage of the knowledge regarding surface melting taking place presumably at the equilibrium point, we can readily estimate the approximate range of the lower bound of superheating obtained at moderate incident energy densities (i.e., at conditions similar to those encountered in Figure 1). Specifically, and as described below, this simple numerical exercise examines the temperature profile of the solid film corresponding to the very moments at which the surface temperature reaches the melting point; as such, it involves heating only of solid Si, and can, therefore, be performed without having to invoke melting (and subsequently introducing additional approximations, parameters, and complications). First, we list some important features and assumptions of our lower-bound analysis: (1) the use of temperature-dependent thermal and optical material parameters (i.e., heat capacity (c_p) [17-19], thermal conductivity (κ_T) [18,20-21], normal-incidence reflectance (R) [21], and normal-incidence absorption coefficient (α) [22]); (2) the use of experimentally extracted time-dependent intensity profile of the beam; (3) disregarding radiative and convective heat loss to the environment; (4) the assumption of a one-dimensional heat flow scenario in the irradiated/probed area; and (5) disregarding the possibly non-trivial thermal resistance at the Si/SiO_2 interface [23] (inclusion of which would actually further increase the calculated degree of superheating). With the above simplifications, the thermal evolution in the beam-irradiated solid Si can be described as

$$c_p(T)\frac{dT}{dt} = \frac{\partial}{\partial x}\left(\kappa_T(T)\frac{\partial T}{\partial x}\right) + Q' \tag{1.1}$$

where x is the position into the film (with the top surface defined at $x = 0$ and the Si/SiO_2 interface defined at $x = d_{film}$, where d_{film} is the film thickness), T is the temperature, c_p is the heat capacity, κ_T is the thermal conductivity, t is time, and Q' is the internal heat source term applicable at the point of consideration, and is determined by the energy deposition of the incident excimer-laser beam; it can thus be expressed as

$$Q'(x,T) = I_0(t)|\tau(T)|^2[1-\exp[-\alpha(T)dx]\left(\exp\,-\int_{d_{film}}^{0}\alpha(T)dx\right) \tag{1.2}$$

where I_0 is the beam intensity, $|\tau|^2$ is the absorption factor, and α is the absorption coefficient. The heat flow in the quartz substrate is handled by a simple one-dimensional equation without any heat source terms within the substrate.

By numerically solving equation (1) via a finite difference analysis scheme [18], and by identifying the temperatures at the bottom Si/SiO_2 interface and at the top surface precisely corresponding to the moment at which the temperature of the surface reaches the equilibrium melting point, for an incident energy density of 800 mJ/cm^2 (~1.2 CMT), we identify the degree of superheating attained in the Si along the bottom Si/SiO_2 interface to be ~100 K. Note that a higher degree of superheating will take place as the energy density increases (e.g. at 1.5 CMT, the surface-melting-point-defined lower bound superheating is ~150 K). In fact, the temperature at the interface continues to increase as melting initiates and proceeds into the superheated film. For that matter, the actual maximum achievable superheating value is expected to take place at significantly higher energy densities (with increasing energy-deposition/heating rates and greater

temperature gradients within the film), when the degree of superheating at the bottom interface becomes sufficiently large to actually trigger melting of solid at the interface; this is indeed what is observed experimentally, and we are presently carrying out a series of such experiments as well as executing the melting-transition-incorporating numerical analysis to accurately identify the maximum superheating in the film. Preliminary findings indicate that melting is initiated at or near the interface at much higher temperatures than the lower-bound numbers presented in this paper.

While the superheating of defect-free single-crystal subsurface solid via internal heating is expected based on theoretical considerations of homogeneous nucleation and other intrinsic melting models [24], a substantial degree of superheating taking place at the buried interface between crystal Si and amorphous SiO_2 may be viewed as an occurrence which is less expected. Thermodynamically, this observation of the melt-resistant nature of Si at the interface does mean that (1) the interfacial energy of the (100)-Si/SiO_2 interface must be sufficiently low (i.e., less than the sum of liquid-Si/SiO_2 and (100)-Si/liquid-Si interfacial energies) to prohibit either pre-melting [25] or barrier-less liquid nucleation to take place at the interface, and (2) the combined nucleation-resisting effects (arising from the relevant interfacial and elastic strain energies [26]) associated with nucleating a liquid either heterogeneously or homogeneously, at or near the interface, respectively, are significant enough to kinetically permit sustained superheating of Si at the bottom (100)-Si/SiO_2 interface.

The present finding regarding the relatively melt-resistant nature of Si at the bottom oxide interface bodes well for those melting and solidification models [1,3,4,27] that implicitly rely on such a tendency to account for the evolution in microstructure. As mentioned previously, more involved experiments and numerical analysis on superheating and melting of Si along the (100)-Si/SiO_2 interface, as well as at grain boundaries in polycrystalline Si films are presently being conducted, and the findings will be presented elsewhere [28].

CONCLUSIONS

In summary, by utilizing a unique combination of experimental elements and capabilities, we were able to induce and detect substantial superheating of Si at and near the bottom Si/SiO_2 interface during back-side excimer-laser irradiation of (100)-oriented single-crystal Si film on quartz. Using the free surface melting taking place at the equilibrium temperature as the anchoring point, a simple lower-bound solid-phase-only heating analysis corresponding to a rather moderate energy density was performed to reveal that, even for such a case, a substantial degree of superheating (in excess of 100 K) takes place at the interface.

ACKNOWLEDGEMENTS

The authors thank Prof. Mike Thompson of Cornell University for discussion as well as providing the samples used in the present investigation and Mr. Adrian Chitu of Columbia University for discussion regarding the experimental apparatus.

REFERENCES

1. J.S. Im, H.J. Kim, and M.O. Thompson, Appl. Phys. Lett. **63** 1969 (1993)
2. T. Sameshima and S. Usui, Mat. Res. Soc. Symp. Proc. **71** 435 (1986)
3. H. J. Kim and J.S. Im, Mat. Res. Soc. Symp. Proc., **321** 665 (1994)

4. J.S. Im, M. Chahal, P.C. van der Wilt, U.J. Chung, G.S. Ganot, A.M. Chitu, N. Kobayashi, K. Ohmori, and A.B. Limanov, J. Cryst. Growth **312** 2775-2778 (2010)
5. J.S. Im, Mater. Res. Soc. Symp. **1426** 239 (2012)
6. D. Van Gestel, M. Chahal, P. C. van der Wilt, Q. Yu, I. Gordon, J.S. Im, and J. Poortmans, 35th IEEE Photovoltaic Specialists Conference (PVSC) 279 (2010)
7. D.P. Gosain, A. Machida, T. Fujino, Y. Hitsuda, and K. Nakano, J. Sato, Jpn. J. Appl. Phys. **42** L135 (2003)
8. J.S. Im and H.J. Kim, Appl. Phys. Lett. **64** 2303 (1994)
9. E. Rie, Ph.D. Dissertation, University of Vienna (1920)
10. F. Meissner, Zeitschrift fur anorganische und allgemeine Chemie **110** 169 (1920)
11. Q.S. Mei and K. Lu, Prog. Mater. Sci. 1175 (2007)
12. K.F. Kelton and A.L. Greer, Nucleation in Condensed Matter, Pergamon press, 1st ed., 528 (2010)
13. D.H. Auston, C.M. Surko, T.N.C. Venkatesan, R.E. Slusher, and J.A. Golovchenko, Appl. Phys. Lett. **33** 437 (1978)
14. H.A. Atwater, C.V. Thompson, and H.I. Smith, J. Mater. Res. **3** 1232 (1988)
15. H.A. Macleod, Thin-Film Optical Filters, CRC Press 4th ed., Ch. 2 (2010)
16. K. Murakami, K. Kawabe, K. Gamo, S. Namba, and Y. Aoyagi, Phys. Lett. A **70** 332 (1979)
17. P.D. Desai, J. Phys. Chem. Ref. Data **15** 967 (1986)
18. J.P. Leonard, Ph.D. Dissertation, Columbia University (2000)
19. K.K. Kelley, U. S. Bureau Mines Bull. 584, Washington (1960)
20. C.J. Glassbrenner and G.A. Slack, Phys. Rev. **134** 4A A1058 (1969)
21. O.A. Sergeev, A. G. Shashkov, and A. S. Umanskii, Thermophysical Properties of Quartz Glass, Plenum Publishing Corporation 1375 (1983)
22. G.E. Jellison, Jr., and F.A. Modine, J. Appl. Phys. **76** 3758 (1994)
23. D.H. Hurley, M. Khafizov, and S.L. Shinde, J. Appl. Phys. **109** 083504 (2011)
24. K. Lu and Y. Li, Phys. Rev. Lett. 80, 4474 (1998)
25. J.W.M. Frenken and J.F. van der Veen, Phys. Rev. Lett. **54** 134 (1985)
26. D.R. Uhlmann, J. Non-Cryst. Mat. **41** 347 (1980)
27. M. Chahal, P. C. van der Wilt, D. Van Gestel, A.B. Limanov, A.M. Chitu, and J.S. Im, Mater. Res. Soc. Symp. Proc. **1426** 257 (2012)
28. J.J.Wang, Ph.D. Dissertation, Columbia University (2015) [Manuscript in preparation]